Solid-Phase Synthesis and Martensite Transformations in Thin Films

L. V. BYKOVA[1], V. G. MYAGKOV[1] and G. N. BONDARENKO[2]

[1]*Kirensky Institute of Physics, Siberian Branch of the Russian Academy of Sciences, Akademgorodok, Krasnoyarsk 660036 (Russia)*

E-mail: miagkov@iph.krasn.ru

[2]*Institute of Chemistry and Chemical Technology, Siberian Branch of the Russian Academy of Sciences, Ul. K. Marksa 42, Krasnoyarsk 660049 (Russia)*

Abstract

This paper presents experimental data on solid-phase synthesis in double-layer thin-film systems. The rule of the first phase formed at the interface of film reagents at elevated temperatures of annealing is formulated for solid-phase reactions determined by martensite transformations. The temperature at which synthesis is initiated in Ni–Ti, Cd–Au, and Al–Ni films coincides with the temperature of the back martensite transition in NiTi, AuCd, and AlNi alloys so that martensite phases are formed in the reaction products. The first phase rule was also verified for solid-phase synthesis in Cd–Ag, Ni–Mn, FeMn, and Au–Mn systems. In thin films, low-energy processes initiate solid-phase reactions associated with martensite transformations, mass transfer of reagents being up to 200 nm. The martensite model of atomic transfer through the reaction product during solid-phase synthesis in thin films is considered. Martensite shifts can play the dominant role in mass transfer of reagents through the reaction product. It is assumed that the first phase initially formed at the interface of film reagents is formed irrespective of the mode of solid-phase synthesis initiation.

INTRODUCTION

Investigation of solid-phase reactions in thin films showed that when the annealing temperature is raised, the *first phase* is initially formed on the boundary between the films (see, *e.g.*, [1–10]). As the annealing temperature increases, other phases can form in sequence. Predicting the first phase and revealing the tendencies underlying the formation of a phase sequence are the key problems in solid-phase thin-film synthesis. Variations of first phase formation are presented elsewhere [3–10], and new alternatives are being offered, but they do not cover the whole diversity of experimental data.

Previously we showed that solid-phase reactions in thin metal films can occur in the autowave mode if heating is performed at high rates. By analogy with self-propagating high-temperature synthesis (SHS) on powders this mode was called thin-film SHS [11, 12]. For many double-layer films and multilayer samples, the temperatures T_0 of solid-phase reaction initiation are from 400 to 800 K. Comparative analysis of bulky samples with the help of binary phase equilibrium diagrams points to many solid-phase structural transformations occurring in this temperature range. This gave us grounds to assume that the temperatures of solid-phase reaction initiation coincide with the temperatures of solid-phase transformations in reaction products. Indeed, we showed that in the S–Fe binary film system, solid-phase reaction starts at a temperature that coincides with the temperature of the metal–dielectric transition in FeS $\{T_0(\text{S–Fe}) = T_K(\text{FeS})\}$[13]. The relationship between SHS in thin metal films and the order-disorder transition in Au–Cu, Ni–Zn, Cu–Al, and Cu–Zn systems have been studied [14, 15]. It was shown that in Cu–Au, Ni–Zn, Cu–Al, and Cu–Zn binary film systems

the temperatures of SHS initiation are determined by the Kurnakov temperatures T_K for superstructures formed in the reaction products [14, 15]. The first phase and its initiation temperature T_0 were redefined based on these experimental data.

1. The phase with the lowest temperature T_K of a structural phase transition (according to the phase diagram) is the first phase formed at the interface between film condensates

2 . The initiation temperature T_0 of a solid-phase reaction in a thin film coincides with the lowest temperature of the solid-phase structural transformation of the first phase ($T_0 = T_K$).

Martensite transitions are diffusion-free solid-phase transformations during which the collective coherent motion of atoms makes the atoms pass (without bond cleavage) from austenite to martensite phase. Consequently, compounds can hardly form at the martensite transition temperature. Experimental data given in this work, however, prove that synthesis is initiated at the temperature of back martensite transformation and forms martensite phases in the reaction products.

In NiTi, AuCd, NiAl, AgCd, AuMn, NiMn, and FeMn alloys, martensite transformations occur at low temperatures, which are well established. These alloys were used for comparative analysis of the relationship between solid-phase synthesis in Ni–Ti, Au–Cd, Ni–Al, Ag–Cd, Au–Mn, Ni–Mn, and Fe–Mn binary film systems with martensite transformations in reaction products.

EXPERIMENTAL

To obtain binary film systems for investigating solid-phase synthesis in them we employed vacuum and ion plasma deposition methods. Polycrystalline films were obtained by deposition on amorphous cover glass; single crystal samples were prepared by deposition on the freshly cleaved (001) surface of MgO and NaCl ionic crystals. Single crystal films grow on the (001) surface of MgO and NaCl only at temperatures above the epitaxial temperature. For most films, the epitaxial temperature varied from 420 to 520 K. To check the single crystal character of the films we employed transmission electron microscopy and X-ray diffraction; saturation magnetization and the first constant of magnetic anisotropy for film samples were compared with the literature values of these characteristics for bulk samples. To obtain a double-layer film system avoiding solid-phase synthesis during deposition, the second upper layer was deposited at room temperature. To reduce heat losses, the support was as thin as possible, its thickness being 0.10–0.18 mm for glass and mica supports and 0.35–0.40 mm for MgO supports.

To measure the conversion η (if one of the films of the binary film system is ferromagnetic) we employed the torque method. The conversion was defined as the ratio of the magnetic volume of the changed ferromagnetic layer to the initial magnetic volume. The mechanical torque was measured on a rotating anisometer. The torque technique was also used to evaluate magneto-crystallographic anisotropy and saturation magnetization [16]. The chemical composition and thickness of the films were determined by X-ray fluorescence analysis without sample decomposition. Measurements were performed on a Spark-1 spectrometer. The relative error in thickness measurements was 5 %.

The phase composition of the films was analyzed and the interplanar distances were determined by X-ray diffraction analysis on a DRON-4M instrument (CuK_α radiation, $\lambda = 0.154$ nm).

For solid-phase synthesis, the samples were placed on a tungsten heater in a vacuum of ~10 10^{-15} Torr and heated at a rate of at least 20 K/s to the reaction initiation temperature T_0. For reactions in the autowave mode, the samples were cooled at a rate of ~10 K/s after the visually observed reaction front had passed through the sample. When the reaction front moved too slowly (if at all – in the reaction diffusion mode), the samples were subjected to fast thermal annealing (FTA). Fast thermal annealing included heating of two-layer samples to the required temperature at a rate of at least 20 K/s and storage at that temperature for 15 s with subsequent cooling at a rate of ~10 K/s.

RESULTS AND DISCUSSION

Solid-phase synthesis and martensite transformations in Ni—Ti film systems

It is known, that NiTi intermetallide (nitinol) has a shape memory effect due to the martensite transformation, which has the lowest transition temperature among solid-phase transformations (temperature of the start of direct martensite transformation M_S is 340 K, A_S is 360 K) [17].

The Ni/Ti double-layer films deposited on glass supports were experimentally investigated by ion plasma, spraying at support temperatures T_S of 300 K (series 1) and 420 K (series 2). According to the phase diagram, in the temperature range 300–420 K, the Ni–Ti system has no structural phase transformations other than martensite transformations.

The diffractograms obtained for samples from series 1 (Fig. 1, *a*) contain reflections only from nickel and titanium layers. This confirms the assumption that deposition forms only a two-layer film system of nickel and titanium layers. In samples from series 2, however, the compound form at the boundary between nickel and titanium (see Fig. 1, *b*). X-ray diffractograms for series 2 indicate that the reaction products show reflections from unchanged nickel and reflections that may be assigned to the β_2(NiTi) austenite phase, β_{19} and β'_{19} martensite phases, and the Ni_3Ti_4 metastable phase.

The dependence of electric resistance R on the support temperature T_S is nonmonotonous (Fig. 2) and is typical for bulky titanium nickelide and for multilayer film samples [17, 18]. The nonmonotonous character of $R(T_S)$ confirms that the reaction products mainly have martensite phases.

The Ni/Ti double-layer film samples obtained at a temperature T_S equal to 300 K were subjected to FTA. After each FTA cycle, the thickness of the unchanged nickel layer was measured. Figure 3 shows the dependence of the thickness of a layer of changed nickel d(Ni) on the support temperature T_S. The thickness d(Ni) being proportional to the reaction rate, the activation energy E_a was determined from the dependence of d(Ni) on T_S (20 kJ/mol). From this dependence it follows that formation of compounds at the interface between nickel and titanium starts at T_S ~ 400 K.

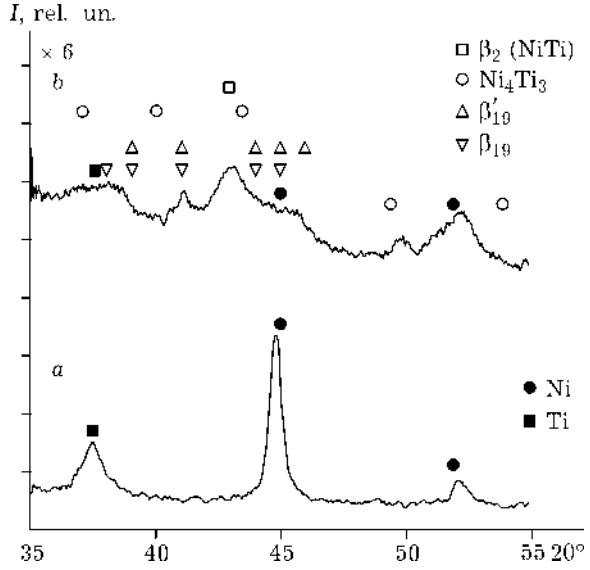

Fig. 1. Diffractograms of the Ti(90 nm)/Ni(75 nm) binary film sample after sequential deposition of a titanium layer on a nickel layer at support temperatures: *a* – T_S = 300 K (before reaction), *b* – T_S = 420 K (after reaction).

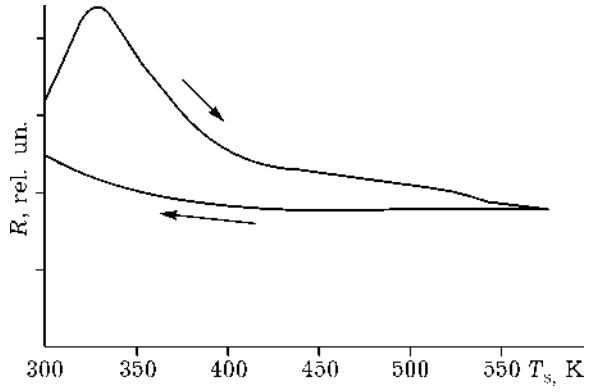

Fig. 2. Dependence of the relative electric resistance R of the Ti(90 nm)/Ni(75 nm) binary film sample, where 40 nm of nickel reacted, on the support temperature T_S.

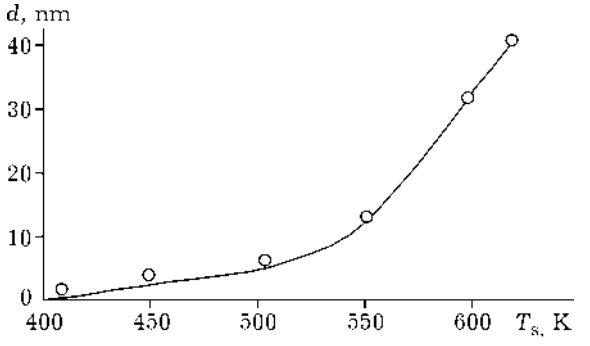

Fig. 3. Dependence of the thickness d(Ni) of changed nickel in the Ti(110 nm)/Ni(50 nm) binary film sample on the support temperature T_S in the fast thermal annealing mode.

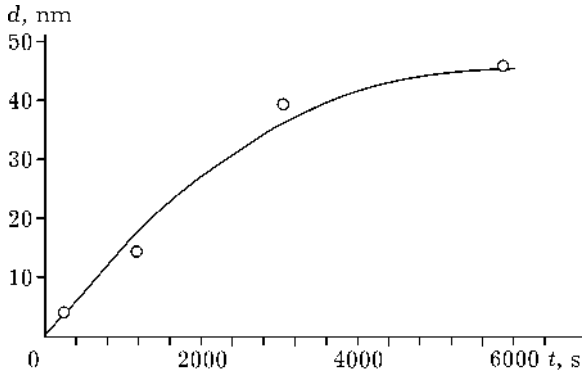

Fig. 4. Dependence of the thickness d(Ni) of changed nickel in the Ti(110 nm)/Ni(50 nm) binary film sample on the annealing time. T_S = 400 K.

The diffusion coefficient D was calculated from the dependence of d(Ni) on the annealing time for T_S = 420 K (Fig. 4), which is close to the parabolic law $d^2(\text{Ni}) \sim Dt$. The coefficient was found to be ~0.5 10^{-18} m^2/s, which is close to the diffusion coefficient at the boundaries of grains.

The low activation energy E_a and the similarity between the diffusion coefficient D and the grain boundary diffusion coefficient indicate that nickel and titanium atoms are highly mobile during synthesis.

It follows from experiments that the temperature T_0 of initiation of a solid-phase reaction between the nickel and titanium layers approaches the temperature of the back martensite transformation A_S in titanium nickelide, with martensite phases found among the reaction products.

Solid-phase synthesis and martensite transformations in Cd—Au and Cd—Ag double-layer film systems

Over the last 70 years, martensite phases of the AuCd alloy have attracted the attention of researchers since they possess the shape memory effect and are characterized by deformation to a rubbery state. The nature of the rubbery state in the AuCd alloy is associated with short-range atomic ordering of martensite phases during aging at room temperature [19]. As is known, the b_2 austenite phase experiences two martensite transitions depending on the composition: $\beta_2 \rightarrow \gamma_2'$ and $\beta_2 \rightarrow \zeta_2'$, where γ_2' is the orthorhombic phase for Au–Cd alloy with 47.5 % cadmium and ζ_2' is a trigonal phase with 49–52 % cadmium. γ_2'-Martensite has an orthorhombic lattice, but the atomic positions were corrected more than once, so that now its crystal structure is well established [20]. The structure of ζ_2'-martensite was studied to a less extent. The refined data given in [21] show that the ζ_2' phase has a trigonal unit cell.

The β_2 austenite phase in an Au–Cd alloy with cooling was subjected to a martensite transformation at ~340 K. On the phase equilibrium diagram of the Au–Cd system, this martensite transition has the lowest temperature relative to the temperatures of other solid-phase transformations.

In experiments we used Au–Cd double-layer film samples obtained by vacuum deposition on glass supports and on the freshly cleaved MgO (001) surface. To prevent reaction between the Au and Cd films, the deposition was conducted at room temperature. The typical thickness of the Cd layer was ~100–250 nm, and the thickness of the Au layer was ~50–100 nm. The X-ray diffractogram of the initial sample contained reflections only from gold and cadmium layers (Fig. 5, *a*) and did not change during annealing at 315 K for 150 h.

A solid-phase reaction between the Au and Cd layers was initiated at a temperature T_0 (Au/

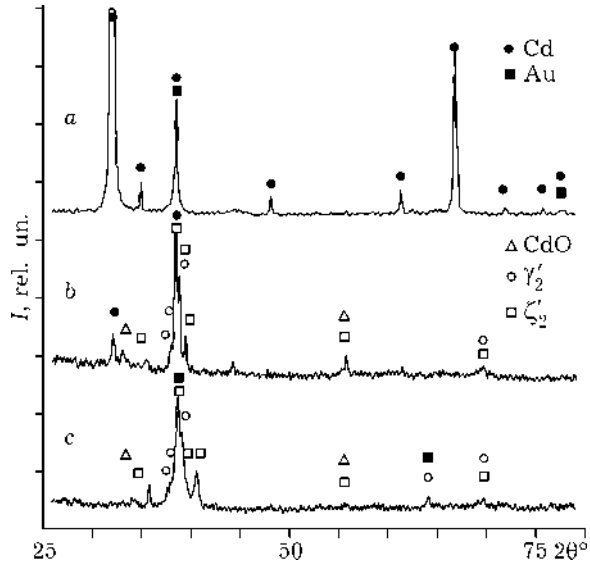

Fig. 5. Diffraction pattern in the Au(80 nm)/Cd(200 nm) film sample: *a* – before reaction; *b* – after SHS wave propagation through the starting sample; *c* – after second initiation of an SHS wave in the changed sample with an Au(80 nm) layer deposited on the upper layer of the sample.

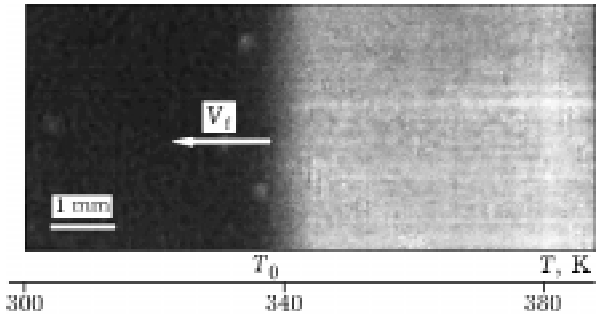

Fig. 6. Photograph of the SHS front propagating in a gradient temperature field in the Au(80 nm)/Cd(200 nm) binary film sample. The ceased motion temperature of the front coincides with the SHS initiation temperature T_0 in the Au(80 nm)/Cd(200 nm) film sample.

Cd) = 340 K and proceeded in the autowave mode; the motion of the reaction front was easily visualized (Fig. 6). The pattern of reaction front propagation is typical for double-layer film samples on which SHS occurs.

After the SHS wave had traveled through the Au/Cd sample, the diffraction pattern changed radically (see Fig. 5, *b*). The intensity of reflections from Au and Cd decreased, which suggested that the reaction occurred between the cadmium and gold layers. Analysis of the diffraction reflections shown in Fig. 5, *b* indicates that the reaction products contain a mixture of γ_2' and ζ_2' martensite phases (dominant products) and an unchanged cadmium layer. The end product is a $(\gamma_2' + \zeta_2')$/Cd double-layer system consisting of a cadmium film adjacent to the support and a $(\gamma_2' + \zeta_2')$ martensite film.

Unexpectedly, it appeared that the reaction may be continued if the upper surface of the $(\gamma_2' + \zeta_2')$/Cd sample is covered with an Au (80 nm) layer. In this Au/$(\gamma_2' + \zeta_2')$/Cd layer system, the reaction is initiated at the same temperature T_0 = 340 K and also occurs as an autowave reaction. After the second SHS front, the diffraction pattern does not change except that the cadmium reflections vanish completely (see Fig. 5, *c*). This suggests that the reaction between the Au and Cd films occurs via the $(\gamma_2' + \zeta_2')$ martensite layer, which serves as a diffusion barrier for the reaction to proceed until the cadmium layer has completely vanished. Indeed, next Au layers applied to the changed samples did not show an SHS wave.

The rate of the SHS front around the initiation temperature is $V_f \sim 1\ 10^{-2}$ m/s. If the reaction is assumed to start at the interface between the film reagents, propagating in the bulk of the sample and along its surface at the same rate, then the diffusion coefficient is $D \sim dV_f = 2\ 10^{-9}$ m^2/s, where d = 200 nm is the layer thickness of the reaction products. This value of the diffusion coefficient is typical for the liquid state. The tipical value of the diffusion coefficient at the boundary of grains in thin films is $D \sim 10^{-17}$ m^2/s.

It is natural to assume that reagents pass into the liquid phase because of significant heat evolution during the reaction. To measure the heat released during reaction front propagation, it was necessary to preliminarily deposit a chromel-copel thermocouple and then an Au(80 nm)/Cd(200 nm) film pair on a glass support. The thermocouple, however, did not show a increase in the temperature of the Au(80 nm)/Cd(200 nm) sample during reaction wave propagation (Fig. 7). This suggests that in the Au/$(\gamma_2' + \zeta_2')$/Cd sample the reaction occurs in the solid phase, since the temperature of the $(\gamma_2' + \zeta_2')$ martensite layer does not differ from the initiation temperature T_0 = 340 K.

The maximal temperature of the reaction front was calculated to be only 600 K (heat loss into environment was neglected). Therefore, this is a solid-phase reaction; this temperature cannot be realized because of heat release into support, as indicated by experiment (see Fig. 7).

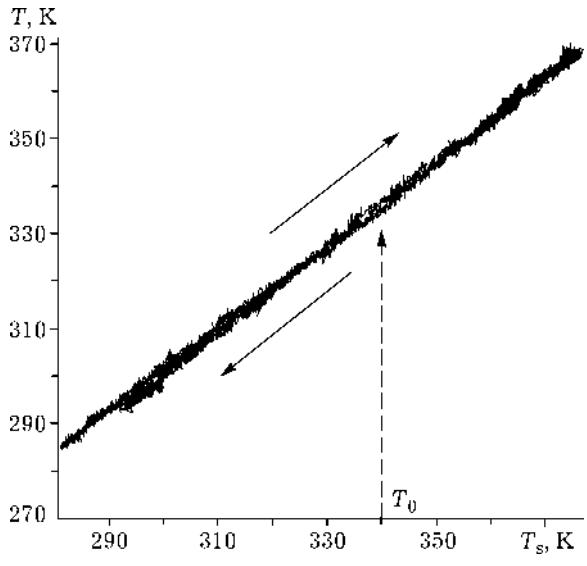

Fig. 7. Film temperature of Au(80 nm)/Cd(200 nm) *versus* support temperature T_S. At T_S = 340 K during SHS wave propagation the film temperature does not increase.

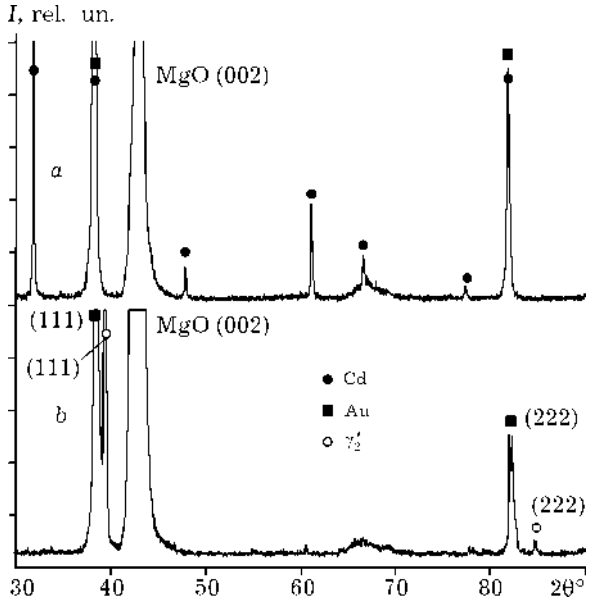

Fig. 8. Diffraction pattern of the Au(80 nm)/Cd(200 nm)/MgO(001) film sample: *a* – before reaction; *b* – after SHS wave propagation through the starting sample.

The threshold character of reaction initiation and the extremely high diffusion coefficient during the low-temperature reaction at the front suggest that grain boundary diffusion is not the major mechanism of mass transfer during reaction wave propagation.

To examine possible routes of ass transfer through the reaction product we studied SHS between the crystalline Cd film and the single crystal Au layer. The gold film grew epitaxially by its Au(111) plane parallel to the MgO(001) plane of the support. The diffractogram of the starting Cd/Au(111)/Mg(001) film sample is shown in Fig. 8, *a*. After SHS wave propagation, the diffraction pattern contained only reflections with interplane distances d_1 = 0.229 nm and d_2 = 0.145 nm (see Fig. 8, *b*). These reflections may be assigned to the peaks of γ_2'(111) (d_1' = 0.2314 nm) and γ_2'(222) (d_2' = 0.1562 nm) martensite. The formation of an epitaxial layer of γ_2' martensite on the Mg(001) surface points to directed and ordered atomic transfer via the reaction product (γ_2'-martensite) during synthesis. This deterministic atomic motion leads to oriented growth that forms orientational relations between reagents and reaction products.

Figure 9, *a* shows the dependence of specific electric conductivity ρ on the support

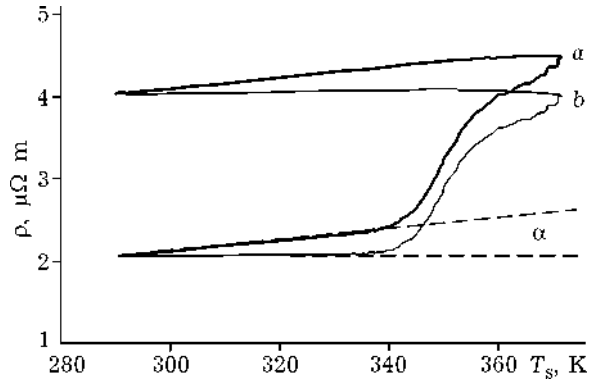

Fig. 9. Dependence of specific electric resistance r on the support temperature T_S for an Au(80 nm)/Cd(200 nm) binary film sample expanded into the temperature dependences of the film material (linear term with the temperature coefficient α (*a*) and synthesis (*b*). Heating rate η = 1 K/s.

temperature T_S for the Au(80 nm)/Cd (200 nm) binary sample (heating rate η = 1 K/s).

The temperature dependence $\rho(T_S)$ has two terms:

$\rho(T_S) = \rho_0(T_S) + \rho^*(T_S)$

where $\rho_0(T_S)$ (linear term with the temperature coefficient α) and $\rho^*(T_S)$ (see Fig. 9, *b*) are the temperature dependences of the film material and synthesis, respectively. The specific resistance of the film material $\rho_0(T_S)$ may be recorded as $\rho_0(T_S) = \rho(290\ \text{K}) + \alpha(T - 290\ \text{K})$ where α is the temperature coefficient of resistance.

Figure 10 presents the plot of the Arrhenius dependence of martensite formation during SHS in the Au(80 nm)/Cd(200 nm) film sample, where $\kappa(T_S)$ is the reaction rate. The reaction activation energies E_1 and E_2 were calculated

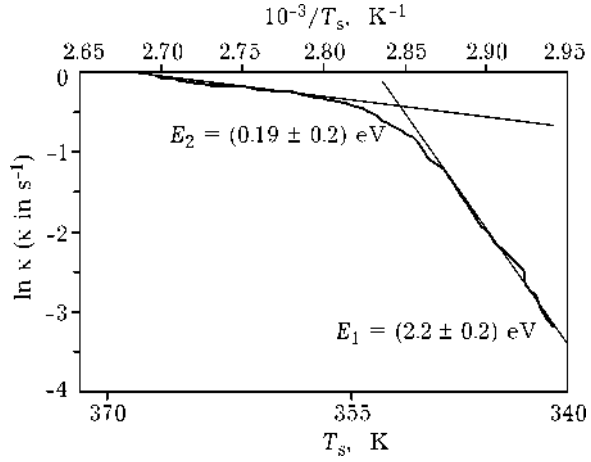

Fig. 10. Plot of the Arrhenius dependence of martensite formation during SHS in an Au(80 nm)/Cd(200 nm) binary film sample.

from the dependence ln $\kappa(1/T_S)$. The wide difference between the experimental values of E_1 and E_2 suggests that solid-phase synthesis in Au/Cd film samples follows different mechanisms. For the temperature range 340–355 K where $E_1 = (2.2 \pm 0.2)$ eV, one can assume that SHS starts with diffusion processes such as recrystallization with increasing size of grains and diffusion along grain boundaries. As the temperature increases to 355–370 K, mass transfer of reagents through reaction products changes radically. The slow diffusion character shifts into a fast avalanche-like collective mechanism of atomic transfer, creating extremely low activation energy $E_2 = (0.19 \pm 0.02)$ eV.

It follows from experiments that the temperature of solid-phase synthesis initiated in Au/Cd binary film samples coincides with the temperature of the back martensite transition, and that the reaction products contain martensite phases [22].

Experiments for Ni/Ti and Au/Cd film systems permit us to formulate the rule of first phase formation in binary film condensates for the case of martensite transitions with the lowest temperature among solid-phase transformations:

a) the phase with the lowest (according to phase equilibrium diagram) temperature of structural phase transformation is the first phase formed at the interface between two film condensates;

b) if this structural phase transformation is a martensite transformation, the starting temperature T_0 of a solid-phase reaction in thin films coincides with the temperature of the start of the reverse martensite transformation A_S ($T_0 = A_S$), and the reaction products contain the austenite and martensite phases.

Since martensite transformations can determine solid-phase reactions, the chemical and structural mechanisms of these transformations are expected to be identical. The mechanism of atomic transfer during martensite type reactions is anticipated to be as follows. As a result of chemisorption, the initial boundary between film reagents is a 2*D* reaction product (martensite). As is known, numerous metals and alloys liable to undergo martensite transformations and having a β_2 *bcc* lattice lose structure stability with respect to the $\{110\}\langle 1\bar{1}0\rangle$ shift at martensite transformation temperatures [23, 24], which is associated with a decrease in the shift module $G' = (C_{11} - C_{12})/2 \to 0$. When the sample temperature increases to the back martensite transformation temperature, martensite is converted into austenite. The intense strains arising during the transformation make reagent atoms approach each other and decrease the activation energy, initiating the reaction. Thin film reactions initiated by martensite transformations are believed to be directed cooperative reactions with reagent atoms moving through the reaction product (austenite) in a direction perpendicular to the plane of the film and coinciding with the nearest $\{110\}\langle 1\bar{1}0\rangle$ type direction of the martensite shift. Figure 11 shows an approximate scheme of atomic motion during the reaction associated with the martensite transformation.

A distinction of the Cd–Ag system lies in the fact that the martensite transition temperature of an AgCd alloy is below room temperature [25]. Consequently, according to the suggested first phase formation rule, solid-phase synthesis in Cd–Ag binary film systems is ex-

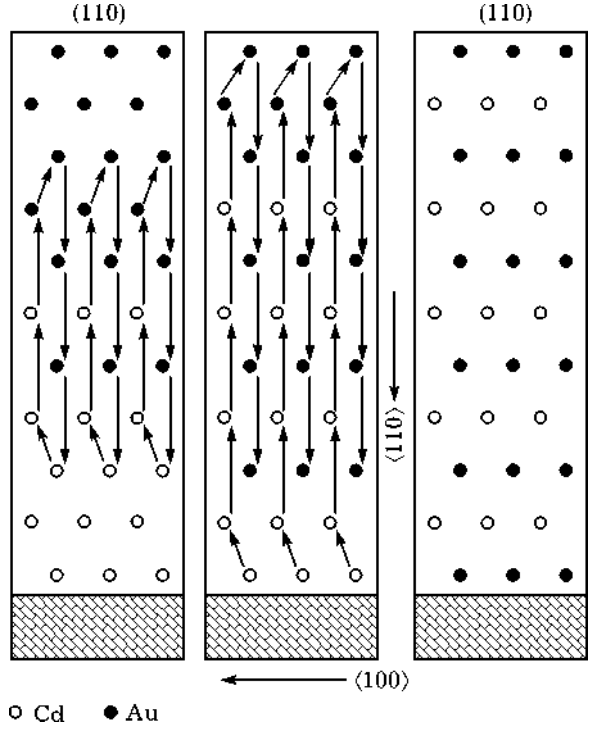

Fig. 11. Hypothetical scheme of atomic motion during solid-phase reaction associated with the martensite transformation. The atoms move in the $\langle 1\bar{1}0\rangle$ direction in the (110) plane.

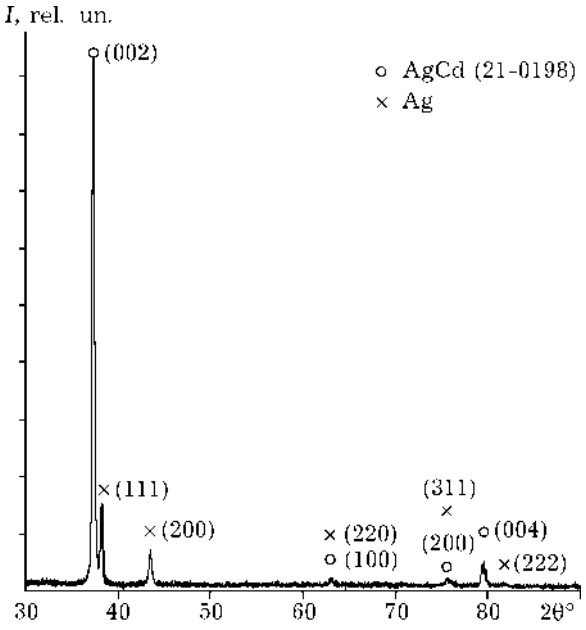

Fig. 12. Diffraction pattern of sequential deposition of Ag(100 nm) and Cd(100 nm) layers on a glass support at room temperature.

pected to occur during deposition. Indeed, as shown by experimental data, solid-phase synthesis in Cd/Ag films occurs at room temperature during deposition, forming an AgCd alloy (austenite), as confirmed by the diffraction pattern of Cd/Ag samples (Fig. 12).

Self-propagating high-temperature synthesis and martensite transformations in Al—Ni film systems

A number of publications deal with solid-phase synthesis in multilayers and Al/Ni binary thin films [26–32]. The phase diagram of the Al–Ni system shows that there are five intermetallic phases: Al_3Ni, Al_3Ni_2, AlNi, Al_3Ni_5, $AlNi_3$. The majority of studies indicate that Al_3Ni is the first phase formed at the Al/Ni interface at elevated temperatures (~573 K). However, this may be preceded by a metastable phase η-Al_9Ni_2. Some authors admit that the AlNi phase can form in the temperature range in which the Al_3Ni phase can exist. In Al/Ni films subjected to ion irradiation and mechanochemical treatment, amorphization can take place. Cold rolling of Al/Ni multilayer foil with varying composition results in a complete transformation of the samples into Al_3Ni and AlNi phases. Previously, we showed that at high

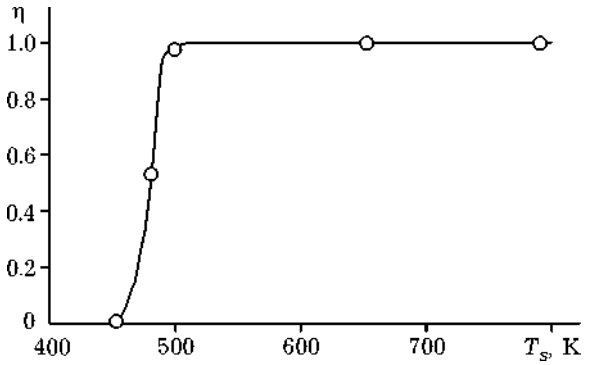

Fig. 13. Dependence of conversion η on the support temperature T_S during SHS in Ni/Al binary films.

heating rates, solid-phase synthesis in Al/Ni thin films occurs in the SHS mode [12, 13].

In experiments we used double-layer films samples of Al/Ni prepared by vacuum evaporation o glass supports and on freshly cut-off MgO(001) surface. The dependence of conversion $\eta(T_S)$ during SHS in Ni/Al films shows that the reaction starts at $T_0 \sim 450$ K (Fig. 13). This temperature lies within the range of the reverse martensite transition of the AlNi phase (~410–460 K).

The diffractograms of the Al(100 nm)/Ni(100 nm)/MgO sample recorded in an accumulation mode after SHS front propagation ($\eta = 1$) indicated that the β_2-NiAl phase possibly formed along with martensite phases and their modifications (LI_0 structure, which can have either ABC (3R) or ABCABAC 7R (14 M) packing) [33]. The shape memory effect in the product samples is strong evidence in favor of martensite phases formed during SHS in Ni/Al double-layer thin films (Fig. 14).

A solid-phase reaction between the Al and Ni layers may be initiated by two methods. In the first case, the samples were obtained by deposition of Ni and Al layers on the (001) NaCl surface at 520 K (*i.e.*, above the initiation temperature T_0). I the second method, the Ni film was deposited on the (001) NaCl surface at 520 K, while the Al film was applied at room temperature with further heating of the binary film system to a temperature above T_0. In this case, the reaction occurred in the SHS mode (heating rates were higher than 20 K/s). The resulting sample 2–3 mm in width and 8–12 mm in length were freed from the NaCl support in distilled water and placed on the preliminarily oxidized surface of copper foil. After moisture

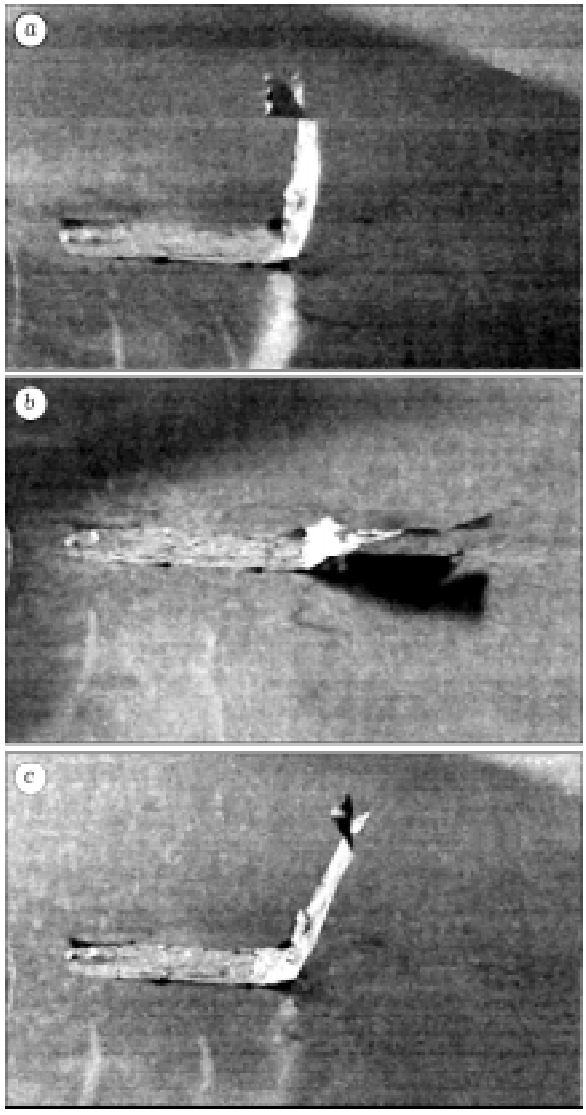

Fig. 14. Reversible shape memory effect in thin Al/Ni films: *a* – starting Al/Ni film sample after solid-phase synthesis deformed at room temperature ~295 K; *b* – after heating to ~520 K; *c* – the same, with subsequent cooling to room temperature.

had been removed at room temperature, one edge of the film was cautiously lifted with a razor blade and deformed in a direction perpendicular to that of the foil plane (see Fig. 14, *a*). When the sample was heated to a temperature above the initiation point (*i.e.*, $T = 520\ \text{K} > T_0$; see Fig. 14, *b*) and further cooled to room temperature (see Fig. 14, *c*), the reversed shape memory effect was observed. After aging for 1 h at room temperature, the sample completely recovered its shape (see Fig. 14, *a*). The reversible shape memory effect was observed in samples where synthesis was initiated by co-deposition and in binary films after SHS. This was found to be a recurrent effect, which does not vanish after aging for 1 month at room temperature [34].

Our studies showed that the initiation temperature of solid-phase synthesis in Ni/Al film samples coincides with the reverse martensite transition temperature of the AlNi phase with martensite phases found among the reaction products. Therefore, unambiguous identification of the first phase after solid-phase synthesis in Al/Ni layers is apparently due to the presence of martensite phases and their forms whose identification presents difficulties. Solid-phase synthesis in Al/Ni thin film systems completely supports the suggested first phase formation rule.

Solid-phase synthesis and martensite transformations in Ni–Mn, Fe–Mn, and Au–Mn binary film systems

Below we give a comparative analysis of the reverse martensite transformation temperatures A_S in FeMn, NiMn, and AuMn alloys and solid-phase synthesis initiation temperatures in Fe–Mn, Ni–Mn, and Au–Mn binary film systems.

In the **Ni–Mn binary system**, a martensite transformation with A_S ~520 K has been found [35].

Our experiments employed Ni/Mn double-layer film samples prepared by vacuum deposition on glass supports. During fast thermal annealing, the reaction starts at ~550 K. Analysis of the diffraction reflections of the changed samples shows that martensite phases possibly formed. Our study revealed a relationship between solid-phase synthesis in Mn/Ni binary film samples and martensite transformations in the Ni–Mn system.

Au–Mn system. As is known for AuMn alloys, the $\beta \rightarrow \beta_1'$ martensite transformation temperature is 505 K [36]. The first phase rule suggests that solid-phase synthesis in Mn/Au films is initiated by film deposition if the support temperature is above the temperature T_K of the $\beta \rightarrow \beta_1'$ martensite transition (above 505 K).

Solid-phase synthesis occurred during the deposition of a manganese layer (~100 nm thick)on an Au(111)/MgO(001) single crystal film

heated to ~570 K. The diffraction pattern off the Mn/Au (111)/MgO(001) binary film sample recorded after synthesis showed that martensite phases were present among the reaction products.

The presence of martensite phases among the reaction products and the fact that T_0 (<570 K) approximated A_S ~500 K (the lowest temperature of solid-phase transformations in Mn–Au systems) imply that martensite transformations dominate in solid-phase synthesis in Mn/Au binary films. These data are consistent with the proposed first phase rule.

The Fe–Mn system does not form compounds; consequently, manganese and iron should not react with each other. For the Fe–24Mn alloy, however, martensite transitions (MTs) have been reported [37, 38]. As is known, $\gamma \rightarrow \varepsilon$ MTs underlie the shape memory effect for alloys based on the Fe–M system, and the temperature of the reverse martensite transformation A_S is ~490 K. No data are available on solid-phase synthesis in Fe/Mn binary films.

In experiment we used Mn/Fe double-layer film samples prepared by sequential vacuum deposition of iron and manganese on glass and mica supports and on a freshly cut-off MgO(001) surface.

During fast thermal annealing, solid-phase synthesis started at T_0 ~ 550 K. It follows from magnetometric measurements that at T_0~550 K 12.5 nm of iron reacts within 1 min. This corresponds to the diffusion coefficient $D \sim 2\ 10^{-18}$ m^2/s, indicating that Fe and Mn atoms are highly mobile during synthesis at ~550 K.

After a manganese layer had been deposited on the Fe(001)/MgO(001) surface at ~570 K, the diffractogram of the sample (Fig. 15) contained a reflection from residual Fe(002) and a new reflection with an interplanar distance $d = 0.221$ nm. Because the Fe–Mn binary system contains no intermetallic compounds, this reflection may belong to ε-martensite alone. The presence of only one ε(110) reflection points to orientated growth of ε-martensite on the Fe(001) surface in accordance with the epitaxial relations ε(110)‖Fe(001).

The presence of ε-martensite among the reaction products and the similarity between the temperature of initiation T_0 (<570 K) and

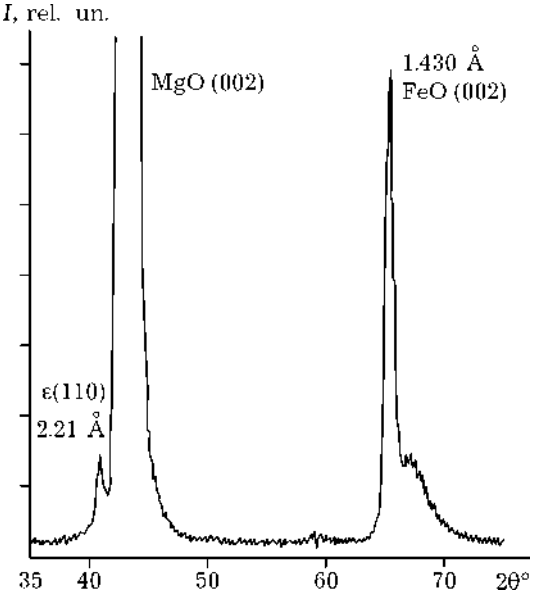

Fig. 15. Diffractogram of the Mn/Fe(001)/MgO(001) sample after an Mn layer has been deposited on the Fe(001)/MgO(001) surface at ~570 K.

reverse martensite transformation $\varepsilon \rightarrow \gamma$ (A_S ~450 K) indicate that martensite transformations in the Fe–24Mn alloy determine solid-phase synthesis in Fe/Mn binary films.

The Ni, Mn, and Au metals have very high melting temperatures ($T_m > 1500$ K) at which the chemical bonds are broken and diffusion becomes sufficiently fast (~10^{-9} m^2/s) for reagents to be mixed. However, we showed that a reaction between these elements is initiated and subsequently occurs at low temperatures (T_0 = 500–600 K). Cleavage of chemical bonds and solid-phase synthesis at low temperatures are associated with the mechanisms of martensite transformations of intermetallic compounds formed as reaction products.

CONCLUSIONS

Our studies of Ni–Ti, Au–Cd, Ni–Al, Ag–Cd, Au–Mn, Ni–Mn, and Fe–Mn double-layer film systems allowed us

1) to formulate the first phase formation rule for solid-phase synthesis in binary film condensates in cases of martensite transformations with the lowest temperature among other structural solid-phase transformations;

2) to propose a martensite type atomic transfer mechanism for the reactions.

A martensite type atomic mechanism is understood as directed atomic motion of reagents through a reaction product (austenite), namely, motion in a direction perpendicular to the plane of the film. The direction of the atomic motion of reagents coincides with the nearest $\{110\}\langle 1\bar{1}0\rangle$ type direction of the martensite shift. This results in a fast transfer of reagent atoms through the reaction product, forming orientation relations between reagents and reaction products.

The martensite mechanism suggests that shear deformations play an extremely important role for initiating solid-phase reactions on the interface between reagents. Therefore, formation of austenite and martensite phases is also expected at the initial stage of impact-wave and mechanical synthesis. Indeed, mechanical aluminum-nickel alloying forms β_2-NiAl [37, 38] and $L1_0$ [39, 40] phases.

It is well known that martensite is formed by mechanical strains. Mechanical load strongly affects the kinetics and temperature of martensite transformations. Consequently, solid-phase reactions with dominant martensite transformations may also be initiated by impact or pressure, leading to the explosive mode of synthesis.

Acknowledgements

This work was supported by the MMK Fund, the Ansferr Centre, and Intels Fund grant No. 10-03−02.

REFERENCES

1 Tonkiye plenki. Vzaimnaya diffuziya i reaktsii, in J. Pote, K. Too and J. Mayer (Eds.), Mir, Moscow, 1982.
2 J. W. Mayer, S. S. Lau, Electronic Material Science: for Integrated Circuits in Si and GaAs, New York, 1990.
3 R. W. Bene, *Appl. Phys. Lett.*, 41 (1982) 529.
4 U. Gosele, K. N. Tu, *J. Appl. Phys.*, 53 (1982) 3252.
5 U. Gosele, K. N. Tu, *Ibid.*, 66 (1989) 2612.
6 F. M. d'Heurle, *J. Mater. Res.*, 1 (1986) 205.
7 W. H. Wang, W. K. Wang, *J. Appl. Phys.*, 76 (1994) 1578.
8 M. Zhang, W. Yu, W. H. Wang, W. K. Wang, *Ibid.*, 80 (1996) 1422.
9 L. A. Clevenger, B. Arcort, W. Ziegler *et al.*, *Ibid.*, 83 (1998) 90.
10 J. J. Hoyt, L. N. Brush, *Ibid.*, 78 (1995) 1589.
11 V. G. Myagkov, L. E. Bykova, *Dokl. AN*, 354 (1997) 777.
12 V. G. Myagkov, V. S. Zhigalov, L. E. Bykova, V. K. Maltsev, *Zh. Tekhn. Fiz.*, 68 (1998) 58.
13 V. G. Myagkov, V. S. Zhigalov, L. E. Bykova *et al.*, *Dokl. AN*, 371 (2000) 763.
14 V. G. Myagkov, V. S. Zhigalov, L. E. Bykova *et al.*, *Pis'ma v ZhTF*, 71 (2000) 268.
15 V. G. Myagkov, L. E. Bykova G. N. Bondarenko *et al.*, *Zh. Tekhn. Fiz.*, 71 (2001) 104.
16 S. Chikazumi, *J. Appl. Phys.*, 32 (1961) 81S.
17 V. N. Khachin, V. G. Pushin, V. V. Kondratyev, Nikelid titana: struktury i svoystva, Nauka, Moscow, 1992.
18 Y. Q. Yang, H. S. Jia, Z. F. Zhang *et al.*, *Mater. Lett.*, 22 (1995) 137.
19 R. W. Cahn, *Nature*, 374 (1995) 120.
20 T. Suzuki, K. Fujimoto, *Scripta Metall.*, 37 (1997) 1525.
21 M. Kogachi, H. Ishibashi, T. Ohba *et al.*, *Ibid.*, 42 (2000) 841.
22 V. G. Myagkov, L. E. Bykova G. N. Bondarenko, *Dokl. AN*, 388 (2003) 844.
23 C. Zener, *Phys. Rev.*, 71 (1947) 846.
24 H. Warlymont, L. Diley, Martensitnye prevrashcheniya v splavakh na osnove medi, serebra i zolota, Nauka, Moscow, 1980.
25 A. Nagasawa, *J. Phys. Soc. Japan*, 35 (1973) 489.
26 H. Sieber, J. S. Park, J. Weissmuller, J. H. Perepezko, *Acta Mater.*, 49 (2001) 1139.
27 A. J. Gavens, D. Van Heerden, A. B. Mann *et al.*, *J. Appl. Phys.*, 87 (2000) 1255.
28 T. Jeske, G. Schmitz, *Scripta Mater.*, 45 (2001) 555.
29 L. Battezzati, P. Pappalepore, F. Durbiano, I. Gallino, *Acta Mater.*, 47 (1999) 1901.
30 V. H. Garcia, P. M. Mors, C. Scherer, *Ibid.*, 48 (2000) 1201.
31 D. Srinivasan, V. Jayaram, P. K. Das, K. Chattopadhyay, *Scripta Mater.*, 38 1998) 857.
32 U. Rothhaar, H. Oechsner, M. Scheib, R. Muller, *Phys. Rev.*, B61 (2000) 974.
33 P. L. Potapov, N. A. Poliakova, V. A. Udovenko, *Scripta Mater.*, 35 (1996) 423.
34 V. G. Myagkov, L. E. Bykova, *Dokl. AN*, 396, 2 (2004) 187.
35 N. M. Matveeva, E. V. Kozlov, Uporyadochennye fazy v metallicheskikh sistemakh, Nauka, Moscow, 1989.
36 A. E. Vol, I. K. Kagan, Stroyeniye i svoystva dvoynykh metallicheskikh sistem, vol. III, Nauka, Moscow, 1976.
37 S. Cites, A. Fernandez Guillermet, M. Sade, *J. Alloys Compd.*, 278 (1998) 231.
38 L. J. Rong, Y. Y. Li, C. X. Shi, *Mater. Lett.*, 24 (1995) 143.
39 M. Atzmon, *Phys. Rev. Lett.*, 64 (1990) 487.
40 V. K. Portnoy, A. M. Blinov, I. A. Tomilin *et al.*, *FMM*, 93 (2002) 42.